

SRF THEORY DEVELOPMENTS FROM THE CENTER FOR BRIGHT BEAMS*

D. B. Liarte[†], T. Arias, D. L. Hall, M. Liepe, J. P. Sethna, N. Sitaraman
 Cornell University, Ithaca, NY, United States of America
 A. Pack, M. K. Transtrum
 Brigham Young University, Provo, UT, USA

Abstract

We present theoretical studies of SRF materials from the Center for Bright Beams. First, we discuss the effects of disorder, inhomogeneities, and materials anisotropy on the maximum parallel surface field that a superconductor can sustain in an SRF cavity, using linear stability in conjunction with Ginzburg-Landau and Eilenberger theory. We connect our disorder mediated vortex nucleation model to current experimental developments of Nb₃Sn and other cavity materials. Second, we use time-dependent Ginzburg-Landau simulations to explore the role of inhomogeneities in nucleating vortices, and discuss the effects of trapped magnetic flux on the residual resistance of weakly-pinned Nb₃Sn cavities. Third, we present first-principles density-functional theory (DFT) calculations to uncover and characterize the key fundamental materials processes underlying the growth of Nb₃Sn. Our calculations give us key information about how, where, and when the observed tin-depleted regions form. Based on this we plan to develop new coating protocols to mitigate the formation of tin depleted regions.

INTRODUCTION

The fundamental limit to the accelerating E -field in an SRF cavity is the ability of the superconductor to resist penetration of the associated magnetic field H (or equivalently B). SRF cavities are routinely run at peak magnetic fields above the maximum field H_{c1} sustainable in equilibrium; there is a metastable regime at higher fields due to an energy barrier at the surface [1]. H_{sh} marks the stability threshold of the Meissner state. In Fig. 1 we show results from linear stability analysis [2], valid near T_c , for H_{sh} as a function of the Ginzburg-Landau parameter κ , the ratio λ/ξ of the London penetration depth λ to the coherence length ξ . Niobium has $\kappa \approx 1.5$, most of the promising new materials have large κ . At lower temperatures, one must move to more sophisticated Eliashberg theories [3], for which H_{sh} is known analytically for large κ ; numerical studies at lower κ are in progress [4]. Broadly speaking, the results so far for isotropic materials appear similar to those of Ginzburg-Landau.

This manuscript will briefly summarize theoretical work on H_{sh} (the threshold of vortex penetration and hence the quench field). First, we discuss the effect of materials anisotropy on H_{sh} [5]. Second, we discuss theoretical estimates of the effect of disorder [6], and preliminary unpub-

* This work was supported by the US National Science Foundation under Award OIA-1549132, the Center for Bright Beams.

[†] dl778@cornell.edu

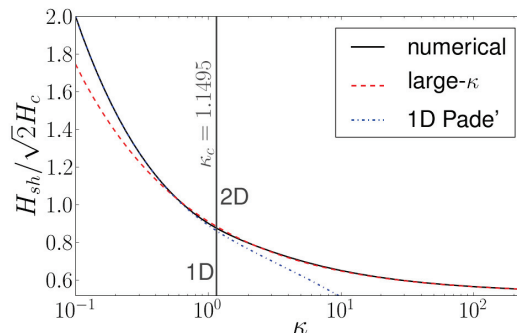


Figure 1: From Ref. [2], showing a numerical estimate of H_{sh} in Ginzburg-Landau theory over many orders of magnitude of κ (black solid line), along with a large- κ expansion (red dashed line), and a Padé approximation for small κ (blue dotted-dashed line).

lished simulations of the effects of surface roughness and materials inhomogeneity. Third, we discuss key practical implications of theoretically calculated point defect energies, interactions, relaxation times, and mobilities in the promising new cavity material Nb₃Sn. Finally, some magnetic flux is trapped in cavities during the cooldown phase, and the response of these flux lines to the oscillating external fields appears to be the dominant source of dissipation in modern cavities. We model potentially important effects of multiple weak-pinning centers on this dissipation due to trapped flux.

THE EFFECT OF MATERIALS ANISOTROPY ON THE MAXIMUM FIELD

Some of the promising new materials are layered, with strongly anisotropic superconducting properties (MgB₂ and the pnictides, for example, but not Nb₃Sn or NbN). Figure 2 illustrates an anisotropic vortex (magnetized region blue, vortex core red) penetrating into the surface of a superconductor (grey). The anisotropy here is characteristic of MgB₂ at low temperatures, except that the vortex core is expanded by a factor of 30 to make it visible.

Near T_c , we find in Ref. [5] that a simple coordinate change and rescaling maps the anisotropic system onto the isotropic case (Fig. 1) above, as studied in Ref. [2]). We find, near T_c where Ginzburg-Landau theory is valid, that H_{sh} is nearly isotropic for large κ materials (Fig. 3. At lower temperatures, different heuristic estimates of the effects of anisotropy on H_{sh} yield conflicting results. Further work at lower temperatures could provide valuable insight into the

Content from this work may be used under the terms of the CC BY 3.0 licence (© 2017). Any distribution of this work must maintain attribution to the author(s), title of the work, publisher, and DOI.

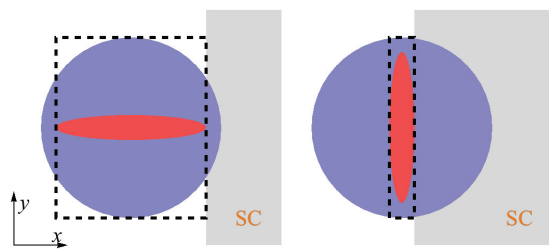


Figure 2: From Ref. [6], showing vortex (blue disk) and vortex core (red disk) of zero-temperature MgB₂ in the *ac* plane, with the external magnetic field parallel to the normal of the plane of the figure. We have drawn the core region about 30 times larger with respect to the penetration depth, so that the core becomes discernible.

possible role of controlled surface orientation for cavities grown from these new materials.

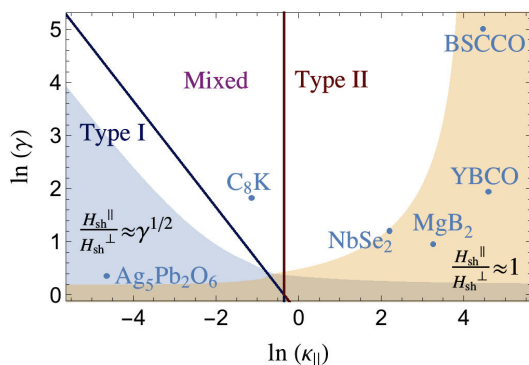


Figure 3: From Ref. [5], showing the phase diagram of anisotropic superconductors in terms of mass anisotropy and GL parameters. The shaded blue and orange regions correspond to regions where the superheating field anisotropy can be approximated by $\gamma^{1/2}$ and 1, respectively, within 10% of accuracy. Note that the superheating field of MgB₂ is nearly isotropic near $T = T_c$.

DISORDER-MEDIATED FLUX ENTRY AND MATERIALS ANISOTROPY

Defect regions and inhomogeneity of superconductor properties can weaken the performance of SRF cavities. In Ref. [5] we used simple estimates based on Bean and Livingston's energy barrier arguments [1], to estimate the effects of disorder in lowering H_{sh} by providing flaws that lower the barrier to vortex penetration. Here we use these calculations to shed light about the relationship between tin depleted regions, low critical temperature profiles, defect sizes and quench fields.

Consider an external magnetic field B , parallel to the surface of a semi-infinite superconductor occupying the half-space $x > 0$. If B is larger than the lower critical field B_{c1} (and smaller than B_{c2}), the vortex lattice phase is thermody-

namically favored. However, if the field is not large enough, a newborn vortex line near the superconductor surface will have to surpass an energy barrier to penetrate the superconductor towards the bulk of the material. This instability typically is surmounted by the simultaneous entry of an entire array of vortices, whose interactions lower one another's barriers. Disorder, in contrast, will lead to a localized region allowing one vortex entry at a time. Bean and Livingston provided simple analytical calculations for the energy barrier felt by one vortex line; we extended their calculation to estimate the dirt needed to reduce this barrier to zero at a quench field $H_q < H_{sh}$.

The new materials have larger κ , and in particular smaller vortex core sizes ξ ; naively one would expect vortex penetration when flaws of size ξ arise. Are these new materials far more sensitive to dirt than niobium? Reassuringly, Figure 4 shows that the low values of the coherence length do not make these new materials substantially more susceptible to disorder-induced vortex penetration [6].

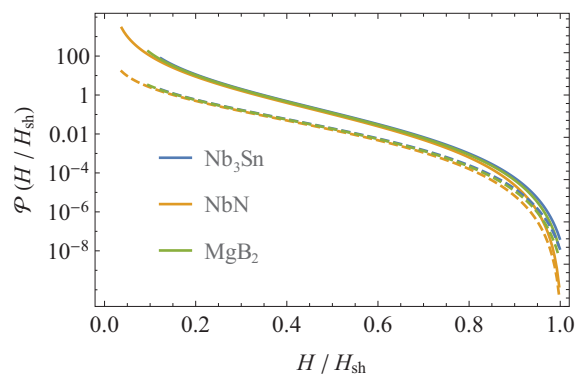


Figure 4: From Ref. [6], showing the reliability of vortex nucleation, in a simple model of Gaussian random disorder, for three candidate superconductors. Solid curves are for a 3D semicircular vortex barrier model; dashed curves are for 2D pancake vortex nucleation in a 2D superconducting layer.

We can use our model to estimate the suppressed superconducting transition temperature T_c^{min} and the flaw depth D_c needed to allow vortex penetration, as a function of H_q (or, in Tesla, B_q) (Fig. 5). For Nb₃Sn we find a flaw size of $D_c \sim 100$ nm and $T_c^{min} \sim 12$ K can allow vortex nucleation and quenches at fields of ~ 77 mT (Fig. 5), consistent with experimental results [7].

TIME-DEPENDENT GINZBURG-LANDAU SIMULATIONS OF ROUGH SURFACES AND DISORDER

To quantify the dependence of H_{sh} on surface roughness and disorder, we have developed a time-dependent Ginzburg-Landau simulation. Figure 6 shows the density $|\psi|^2$ of superconducting electrons at a field just above H_{sh} (top left), showing the entry of several vortices for a 2D system with an irregular surface. On the bottom left, we show the cor-

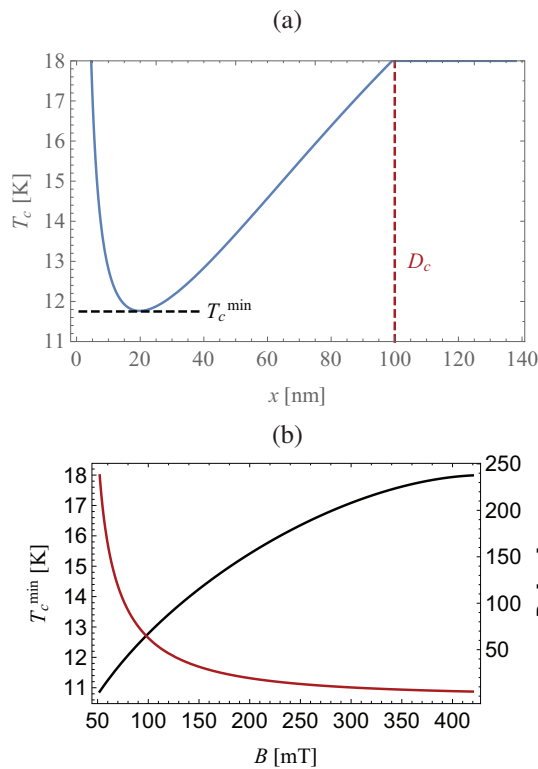


Figure 5: (a) Critical temperature profile that allow nucleation of vortices in Nb₃Sn cavities at a field of ~ 77 mT. (b) Suppressed superconducting transition temperature T_c^{min} (black), and flaw depth D_c (red), as a function of the quench field.

responding supercurrent \mathbf{j} ; on the top right we show the magnetic field H (perpendicular to the plane of the simulation), and on the bottom right we show the effect of surface roughness on $|\psi(\theta)|^2$ around the perimeter. Our initial results quantify how inward-curving regions in the plane perpendicular to the applied field on the perimeter can act as vortex nucleation sites in this geometry. An open question remains what the effect of curvature and surface roughness have when oriented parallel to the applied field.

The effect of roughness in Fig. 6 is to lower H_{sh} by a few percent. By systematically varying the details of the roughness parameters, we can use this tool to identify at what scale roughness will have significant impact on vortex nucleation. SRF cavity roughness can be smoothed to varying degrees. Our TDGL environment can be used to find dangerous regimes or configurations that can have serious consequences for cavity performance.

We can also use this tool as a way to explore vortex dynamics and the effects of pinning sites on trapped residual magnetic flux. Pinning sites originate from inhomogeneities in the material, such as grain boundaries or spatial inhomogeneities in the alloy stoichiometry. By incorporating this information into our TDGL environment we can try to better understand the mechanisms driving residual resistance for typical cavities.

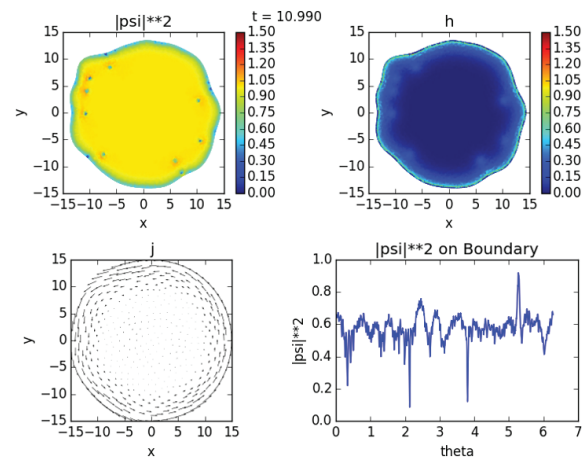


Figure 6: Spatial dependence of the density of superconducting electrons (top left), supercurrent (bottom left), and the induced magnetic field (top right). On the bottom right, we show the variation of the order parameter around the perimeter of the superconductor.

DFT CALCULATIONS

Nb₃Sn cavities are created by depositing tin vapor on the surface of a niobium cavity, which reacts with the niobium to form an irregular surface layer of the compound. Of interest are regions of “tin depleted” Nb₃Sn, known to have a lower superconducting transition temperature than the surrounding Nb₃Sn. These regions may be the nucleation centers responsible for quenches observed well below H_{sh} expected for perfect Nb₃Sn [7].

Density functional theory (DFT) can be used to study layer growth, tin depletion, and other features of Nb₃Sn layers at the single-particle level. This information, combined with experimental data and accounting for the effects of grain boundaries and strain, makes it possible to build a multiscale model of layer growth.

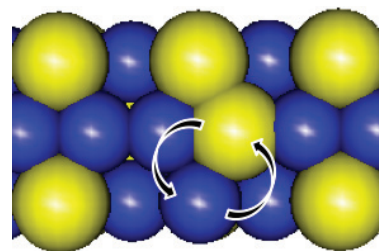


Figure 7: Illustration of antisite disorder. We estimate that on the order of 1% of lattice sites are affected by antisite defects “frozen in” from the high coating temperature. This would make them by far the most common point defect in Nb₃Sn layers.

Our initial work uses in-house DFT software to calculate defect formation and interaction energies, impurity energies, and energy barriers in Nb₃Sn. We have found that antisite disorder (Figure 7), rather than impurities or vacancies, likely sets the electron mean free path in Nb₃Sn and may

Content from this work may be used under the terms of the CC BY 3.0 licence (© 2017). Any distribution of this work must maintain attribution to the author(s), title of the work, publisher, and DOI.

also be responsible for collective weak pinning. We have also found that under certain conditions during growth, it is energetically favorable for Nb₃Sn to form at tin-depleted stoichiometry, while during annealing existing Nb₃Sn near the surface or grain boundaries can become tin-depleted by diffusion (Figure 8). Either or both of these tin depletion mechanisms may result in quench nucleation centers; by understanding them we can for the first time make informed modifications to the coating process in an attempt to limit tin depletion and produce better cavities.

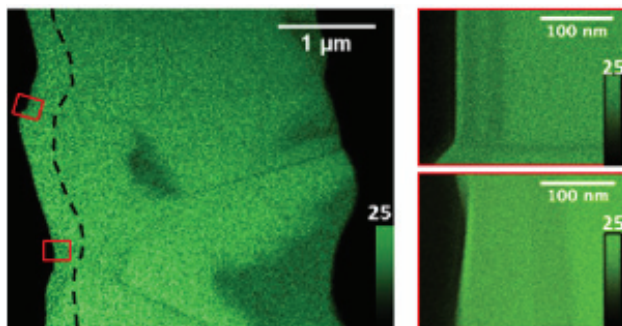


Figure 8: Experimental data showing tin depletion. At left is a tin density map of a layer cross section showing regions of significant (7-8%) tin depletion, in this case mostly deep in the layer relative to the RF penetration depth (dashed line). At right are close ups showing slight (1-2%) tin depletion right at the surface of the layer. Images by Thomas Proslie at Argonne National Lab, received via personal communication with Daniel Hall.

DYNAMICS OF TRAPPED VORTICES; POTENTIAL ROLE OF WEAK PINNING

When the field is high enough for penetration of new vortices, one expects a cascade of vortices leading to a quench. Vortices trapped during the cooling process, while not immediately fatal, do act as sources of residual resistance. Experiments show that the non-BCS surface resistance is proportional to the trapped flux, both for nitrogen-doped Nb cavities [8] and for Nb₃Sn [9]. This suggests that trapped vortices may be a dominant contribution to the quality factor of the cavity.

Previous studies of the residual resistance due to a trapped flux line [10] focused on the Bardeen-Stephen viscous dissipation [11] of a free line pinned a distance below the surface, as the external field drags the line through a otherwise uniform superconducting medium. Experimental measurements in nitrogen-doped Nb cavities showed good agreement to this theory, except that the distance to the pinning center was presumed to change linearly with the mean-free path [8] as it changes due to nitrogen doping. Since nitrogen (or other contaminant gases [12, 13]) should act as weak pinning centers (with many impurities per coherence length cubed), we have been modeling the role of weak pinning in vortex dissipation.

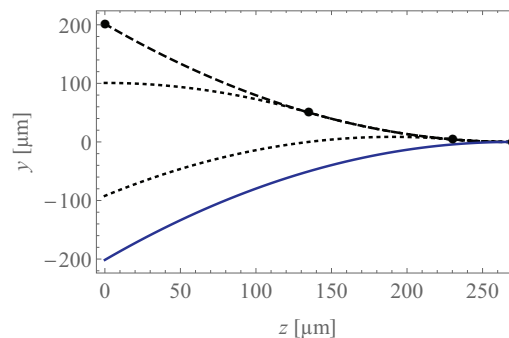


Figure 9: From Ref. [9], showing vortex line solutions at several times, using measured parameters for Nb₃Sn.

Line defects pulled through a disordered medium is one of the classical depinning transitions [14]. The disorder acts as a random potential, and macroscopically there is a threshold force per unit length f_{pin} needed to depin the line and start motion (Fig. 9). This depinning transition is preceded by avalanches of all sizes (local regions of vortex motion) and followed by fluctuations on all scales (jerky motion of the vortex line in space and time). For our initial estimates, we have ignored these fluctuations, using a ‘mean-field’ model where our superconducting vortex line has a threshold supercurrent $j_d \propto f_{pin}^{2/3}$ for motion. We presume also that the energy dissipated is f_{pin} times the area swept out by the vortex as the external surface field pulls it to and fro (Fig. 10).

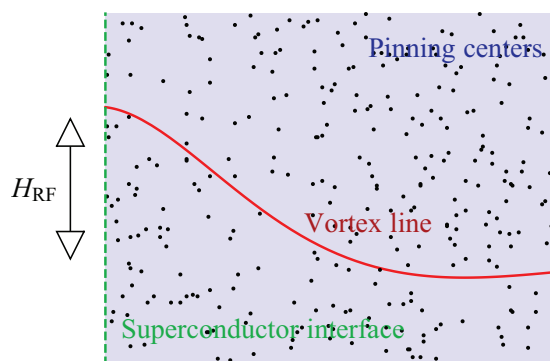


Figure 10: Illustration of a vortex line (red curve) subject to an external rf magnetic field and the collective action of many pinning centers.

The residual resistance measured in Nb₃Sn cavities shows a linear dependence on the peak RF field (Fig. 11, [9]). The scaling properties of the terms included in the earlier work [10] all predict no dependence on the strength of the external oscillating field. Our theory including weak pinning but ignoring the viscous dissipation produces a dissipation that is linear in this external field. Our estimates, however, suggest that our theory should be valid at MHz frequencies, but at the operating GHz frequencies the viscous term must be important for the energy dissipation. Our preliminary

calculations suggest that incorporating both can provide a reasonable explanation of the experimental data, but we still do not obtain quantitative agreement.

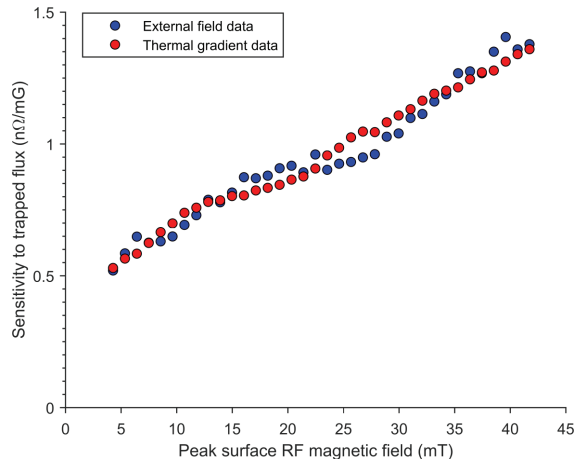


Figure 11: From Ref. [9], showing the sensitivity of residual resistance to trapped magnetic flux, as a function of the peak rf field.

CONCLUSION

The collaboration between scientists inside and outside traditional accelerator physicists made possible by the Center for Bright Beams has been immensely fruitful. This proceedings illustrates the richness of the science at the intersection of accelerator experimentalists working on SRF cavities with condensed-matter physicists with interests in continuum field theories and *ab-initio* electronic structure calculations of materials properties. (One must also note the important contributions of experimental condensed matter physicists in the collaboration.) Current SRF cavities are pushing fundamental limits of superconductors, and are a source of fascinating challenges for theoretical condensed-matter physics. Conversely, we find that theoretical calculations are remarkably fruitful in guiding and interpreting experimental findings.

ACKNOWLEDGMENT

We thank Alex Gurevich for useful conversations.

REFERENCES

- [1] C. P. Bean and J. D. Livingston, “Surface Barrier in Type-II Superconductors” *Phys. Rev. Lett.*, vol. 12, p. 14, 1964.
- [2] M. K. Transtrum, G. Catelani, and J. P. Sethna, “Superheating field of superconductors within Ginzburg-Landau theory” *Phys. Rev. B.*, vol. 83, p. 094505, 2011.

- [3] G. Catelani, and J. P. Sethna, “Temperature dependence of the superheating field for superconductors in the high- κ London limit” *Phys. Rev. B.*, vol. 78, p. 224509, 2008.
- [4] G. Catelani, M. K. Transtrum, and J. P. Sethna, Unpublished.
- [5] D. B. Liarte, M. K. Transtrum, and J. P. Sethna, “Ginzburg-Landau theory of the superheating field anisotropy of layered superconductors” *Phys. Rev. B.*, vol. 94, p. 144505, 2016.
- [6] D. B. Liarte, S. Posen, M. K. Transtrum, G. Catelani, M. Liepe, and J. P. Sethna, “Theoretical estimates of maximum fields in superconducting resonant radio frequency cavities: stability theory, disorder, and laminates”, *Supercond. Sci. Technol.*, vol. 30, p. 033002, 2017.
- [7] D.L. Hall, P. Cueva, D. Liarte, M. Liepe, J.T. Maniscalco, D.A. Muller, R.D. Porter, and J.P. Sethna, “Quench Studies in Single-Cell Nb3Sn Cavities Coated Using Vapour Diffusion”, in *Proc. 8th Int. Particle Accelerator Conf. (IPAC'17)*, Copenhagen, Denmark, May 2017, paper MOPVA116, pp. 1119–1122, <http://jacow.org/ipac2017/papers/mopva116.pdf>, <https://doi.org/10.18429/JACoW-IPAC2017-MOPVA116>, 2017.
- [8] D. Gonnella, J. Kaufman, and M. Liepe, “Impact of nitrogen doping of niobium superconducting cavities on the sensitivity of surface resistance to trapped magnetic flux” *J. Appl. Phys.*, vol. 119, p. 073904, 2016.
- [9] D.L. Hall, D. Liarte, M. Liepe, and J.P. Sethna, “Impact of Trapped Magnetic Flux and Thermal Gradients on the Performance of Nb3Sn Cavities”, in *Proc. 8th Int. Particle Accelerator Conf. (IPAC'17)*, Copenhagen, Denmark, May 2017, paper MOPVA118, pp. 1127–1129, <http://jacow.org/ipac2017/papers/mopva118.pdf>, <https://doi.org/10.18429/JACoW-IPAC2017-MOPVA118>, 2017.
- [10] A. Gurevich and G. Ciovati, “Effect of vortex hotspots on the radio-frequency surface resistance of superconductors” *Phys. Rev. B.*, vol. 87, p. 054502, 2013.
- [11] J. Bardeen and M. J. Stephen, “Theory of the Motion of Vortices in Superconductors” *Phys. Rev.*, vol. 140, p. A1197, 1965.
- [12] P. N. Koufalas, D. L. Hall, M. Liepe, and J. T. Maniscalco, “Effects of interstitial carbon and oxygen on niobium superconducting cavities” *arXiv:1612.08291*, 2016.
- [13] P. N. Koufalas, M. Liepe, and J. T. Maniscalco, “Low temperature doping of niobium cavities: what is really going on?”, presented at the 18th Int. Conf. on RF Superconductivity, Lanzhou, China, paper MOPVA118.
- [14] D. S. Fisher, “Collective transport in random media: from superconductors to earthquakes” *Phys. Rep.*, vol. 301, p. 113, 1998.